MOLECULAR AND CELLULAR BIOLOGY, July 2002, p. 5235–5247 Vol. 22, No. 14
0270-7306/02/$04.00+0 DOI: 10.1128/MCB.22.14.5235–5247.2002

Characterization of Mice Deficient in the Src Family Nonreceptor Tyrosine Kinase Frk/rak

Subhashini Chandrasekharan,[1,2]† Ting Hu Qiu,[2] Nawal Alkharouf,[2] Kelly Brantley,[2] James B. Mitchell,[3] and Edison T. Liu[2]*

Curriculum in Genetics and Molecular Biology, University of North Carolina at Chapel Hill, Chapel Hill, North Carolina 27599[1]; Section of Cell Signaling and Oncogenesis, Division of Clinical Sciences, National Cancer Institute, National Institutes of Health, Gaithersburg, Maryland 20877[2]; and Radiation Biology Branch, National Cancer Institute, National Institutes of Health, Bethesda, Maryland 20892[3]

Received 12 November 2001/Returned for modification 14 January 2002/Accepted 13 March 2002

Frk/rak belongs to a novel family of Src kinases with epithelial tissue-specific expression. Although developmental expression patterns and functional overexpression in vitro have associated these kinases with growth suppression and differentiation, their physiological functions remain largely unknown. We therefore generated mice carrying a null mutation in *iyk*, the mouse homolog of Frk/rak. We report here that *frk*/*rak*$^{-/-}$ mice are viable, show similar growth rates to wild-type animals, and are fertile. Furthermore, a 2-year study of health and survival did not identify differences in the incidence and spectrum of spontaneous tumors or provide evidence of hyperplasias in *frk*/*rak*$^{-/-}$ epithelial tissues. Histological analysis of organs failed to reveal any morphological changes in epithelial tissues that normally express high levels of Frk/rak. Ultrastructural analysis of intestinal enterocytes did not identify defects in brush border morphology or structural polarization, demonstrating that Frk/rak is dispensable for intestinal cytodifferentiation. Additionally, *frk*/*rak*-null mice do not display altered sensitivity to intestinal damage induced by ionizing radiation. cDNA microarray analysis revealed an increase in c-*src* expression and identified subtle changes in the expression of genes regulated by thyroid hormones. Significant decreases in the circulating levels of T3 but not T4 hormone are consistent with this observation and reminiscent of euthyroid sick syndrome, a stress-associated clinical condition.

Protein tyrosine kinases (PTKs) are a large and diverse multigene family evolved to perform functions that regulate a range of cellular processes, including cell growth, differentiation, death, motility, adhesion, and cell-to-cell communication in multicellular organisms. PTKs can be broadly classified into two groups, receptor tyrosine kinases (RTKs) and nonreceptor tyrosine kinases (NRTKs), based on their intracellular locations. RTKs, examples of which include EGFR and PDGFR, have transmembrane domains, which allow them to be integral parts of the plasma membrane and extracellular domains, which are exposed to the external milieu. The extracellular domains bind specific ligands (or growth factors), resulting in activation of the intracellular catalytic kinase domain. The second group of kinases, the NRTKS, possess only the intracellular kinase domain and are usually targeted to the cytoplasmic face of the plasma membrane by N-terminal posttranslational modifications. The Src family kinases (SFKs) are a group of related NRTKs, the prototype of which, c-*src*, was identified as the normal cellular counterpart of the transforming protein v-*src* from the oncogenic Rous sarcoma virus (45). c-*src* encodes a 60-kDa phosphoprotein with kinase activity that is expressed ubiquitously (25). Based on amino acid sequence homology and structural similarity, 7 additional members of this family, Fyn, Yes, Fgr, Hck, Lck, Blk, and Lyn have been isolated. The prototypical SFKs are composed of six structurally and functionally distinct domains called Src homology (SH) domains, which are characterized by specific sequence motifs and regulatory residues (8). The modular structure of the SFKs allows them to interact with a diverse group of proteins, creating highly complex signal transduction networks. SFKs are activated by a variety of extracellular signals and regulate an equally extensive set of cellular functions. SFKs have been demonstrated to be key downstream elements in signaling pathways emerging from RTKs, integrins, cadherins, G protein-coupled receptors, GPI-linked receptors, voltage- (Ca^{2+} and K^{+}) and ligand-gated channels, cytokine receptors, and immune recognition receptors (1, 49). Cellular functions regulated by SFKs include mitosis, cell spreading, adhesion, motility, cell death, survival, and differentiation (49). Further division of the SFKs into groups A and B has been suggested based on their tissue expression profiles. Group A includes Src, Fyn, Hck, and Yes, which are expressed ubiquitously, although with various levels in different cell types. In contrast, SFK group B, consisting of Hck, Fgr, Lck, Blk, and Lyn, is expressed primarily in hematopoietic cells (42).

Less is known about the function of a third group of SFKs, the Frk/rak family of kinases. To date, two genes, *frk*/*rak* and *brk*, which share 60% amino acid homology with one another, have been assigned to this family. These kinases are expressed primarily in epithelial tissues and show the highest homology of ~50% at the amino acid level to Fyn. The first member of

* Corresponding author. Present address: Genome Institute of Singapore, 1 Capricorn 05-01, Science Park II, Singapore 117528, Singapore. Phone: 65-68275212. Fax: 65-68275202. E-mail: gisliue@nus.edu.sg.

† Present address: Department of Cystic Fibrosis and Pulmonary Research, University of North Carolina at Chapel Hill, Chapel Hill, NC 27599-7248.

this family, Rak, was identified in human breast tumors and the mammary epithelial cell line 600PE in a screen for novel tyrosine kinases expressed in breast cancer. The complete cDNA was isolated from the BT-20 cDNA library, and analysis of the primary sequence revealed ~51% identity to Fyn (9). The identical kinase was independently isolated from a human hepatoma cell line (24) and named Frk, an acronym for fyn-related kinase. Chromosomal localization studies reveal that *fyn* and *frk*/*rak* are in fact linked genes located within 1.3 centimorgans of each other on chromosome 6q (11; unpublished data). The mouse homolog *iyk*, an acronym for intestinal tyrosine kinase, was identified as a novel PTK in a screen for SFKs expressed in resting mature mouse mammary glands. The complete cDNA was isolated from 31E-mouse epithelial cells encoding a 57-kDa protein with 89% identity at the amino acid level to Frk/rak (50). This gene was also independently isolated from the mouse insulin-producing cell line β-TC1 and therefore named *bsk*, i.e., beta-cell *src*-like kinase (37). *gtk*, an acronym for gut tyrosine kinase, is the rat homolog of *frk*/*rak* and *iyk* and was identified as a novel *src*-like kinase gene expressed in rat intestinal epithelial cells. The primary structure of Gtk has a 49% homology to fyn and 88% identity to Frk/rak at the amino acid level (16). In the interest of simplicity, both the human gene and its mouse and rat homologs will be referred to as *frk*/*rak* in this report. A related gene, *brk*, breast tumor kinase, was identified as a novel *src*-like kinase expressed in metastatic human breast cancer (32, 33). *brk* encodes a 52-kDa protein with ~60% homology to Frk/rak and ~40% homology to Fyn and Src. The mouse homologue of this kinase, *sik*, was isolated from a mouse duodenum cDNA library and encodes a 52-kDa protein with 80% identity to Brk (53).

Similar to all members of the SFKs, Frk/rak kinases possess the classic SH domain structure and conserved autoregulatory tyrosine residues in their catalytic domains. However, they differ significantly in certain structural features, the most striking of which is the presence of a putative bipartite nuclear localization signal (KRXXXXXFFXXRRR motif) in the SH2 domain. This consensus nuclear localization signal motif is present both in the mouse and rat homologs but not retained in Brk (and its mouse homologue Sik). Consistent with the suggestion that the subcellular localization of these kinases may differ from that of other SFKs, the critical glycine residue in the consensus myristoylation motif MGXXXS/T, necessary for the conjugation of myristate and plasma membrane targeting is absent in human Frk/rak (19). The conserved serine residue (S) is replaced with a glutamine (Q) in Frk/rak at position 6. Furthermore, the consensus motif required for palmitylation (CXXC or CXC) is only partially retained. Taken together, these findings suggest that Frk/rak is unlikely to be targeted to the plasma membrane. Recently, it has been demonstrated that Frk/rak protein is in fact localized to the juxtanuclear region in a number of epithelial cell lines, colocalizing with markers specific to the Golgi (58,000 molecular weight [58K]) and γ-tubulin centrosomal compartments (C. D. Carter, L. D. Miller, and E. T. Liu, unpublished data). The consensus myristoylation sequences are however retained in the mouse and rat homologs (Iyk and Gtk), suggesting potential membrane targeting. In support of this, Gtk is found to be myristoylated in vitro and high kinase activity is detected in the membrane fraction of intestinal epithelial cells, suggesting localization to the plasma membrane (16, 17). Additional distinguishing structural features of Frk/rak are, a 7-amino-acid insert in the SH3 domain (also present in the mouse and rat homologs, Iyk and Gtk) and a conserved DLAARN motif in subdomain VI of the kinase domain found in both members of the family.

The expression profile of Frk/rak and its homologs shows considerable similarity. The expression of *frk*/*rak* is higher in epithelial tissues and cell lines, with the highest expression detected in the kidney and liver (9, 11; C. D. Carter and E. T. Liu, unpublished data). In the mouse, the expression of *frk*/*rak* mRNA was detected primarily in epithelial organs, with highest expression in the intestine, particularly the jejunum and ileum (37, 50). During embryonic development of the rat, expression of Frk/rak in the gut started to increase on day 11 and peaked between days 15 and 18, concomitant with the conversion of the multilayered undifferentiated epithelium to a polarized monolayer (16). Similarly, the highest expression of *brk* and its homolog *sik* are detected in different regions of the gastrointestinal tract, i.e., the stomach, duodenum, and colon (26, 35)

To date, attempts to assign a function to Frk/rak have relied mainly on the study of intracellular localization and the impact of functional overexpression of the gene on growth and differentiation in various cell lines. Surprisingly, and in contrast to prototypical SFKs, overexpression of Frk/rak in a number of cell lines of epithelial and mesenchymal origin resulted in a potent growth arrest (10, 11; R. Craven and L. D. Miller, unpublished observations). Inducible expression of Frk/rak in HeLa cells results in growth suppression, potentially due to an arrest in the G_1 phase of the cell cycle (Carter et al, unpublished data). A putative mechanism is suggested by the observation that Frk/rak was found to associate with hyperphosphorylated and hypophosphorylated forms of retinoblastoma during the G_1 and S phases of the cell cycle in vitro (11). The expression of Frk/rak protein is highest in the G_1 and S phases of the cell cycle and dramatically reduced during mitosis (10, 11). Frk/rak is expressed at the centrosomes during all stages in the cell cycle except mitosis, and expression reappears during the late telophase, suggesting a potential role for Frk/rak in centrosome structure and/or function, particularly in the context of regulation of cell division (C. D. Carter and E. T. Liu, unpublished data). Overexpression of constitutively activated forms of mouse Frk/rak results in suppression of growth of NIH 3T3 fibroblasts and RINm5F pancreatic cells. Cell cycle analysis studies indicate that activated Frk/rak suppresses growth by inducing a G_1 arrest, possibly by preventing entry into the S phase of the cell cycle (3, 38). Interestingly, an increase in the levels of the cdk inhibitor p27 is associated with this growth arrest. Increases in p27 levels have been associated with the differentiation of various cell types and is potentially required for maintenance of the differentiated state (13, 51). A recent study demonstrated increased nerve growth factor-independent neurite growth in PC-12 cells stably expressing wild-type mouse Frk/rak, a process reminiscent of neuronal differentiation (2). The expression of Brk mRNA and protein increases during confluence-induced differentiation of CaCo-2 intestinal epithelial cells (26). The murine homolog, Sik, is rapidly activated upon Ca^{2+}-induced differentiation of mouse

primary keratinocytes, and functional overexpression of wild-type Sik in EMK cells increased the expression of fillagrin, a marker of keratinocyte differentiation (54). Interestingly, genes in invertebrate organisms with the highest similarity to this family of Frk/rak-related kinases are *srk1*, which mediates regeneration in fresh water sponges (39), *stk1* in *Hydra* (7), and *dsrc41*, a *src*-like kinase that regulates ectodermal differentiation in flies (47). Human *frk*/*rak* is localized to 6q21-23 (11), a region that undergoes loss of heterozygosity in 30% of breast cancers and ovarian carcinomas (23, 43). This region has also been defined as a senescence locus by using microcell-mediated chromosome transfer experiments in breast cancer cell lines (35). These observations, in conjunction with in vitro growth-suppressive functions, suggest that *frk*/*rak* is potentially a novel tumor suppressor gene for epithelial cancers regulating growth and/or morphological differentiation of epithelial cells.

In order to investigate these possibilities, we decided to elucidate the physiological function of Frk/rak using gene disruption. In this study we present the characterization of mice bearing a targeted mutation in the mouse *frk*/*rak* gene. We demonstrate that the *frk*/*rak*-null mice are viable and do not show any histological abnormalities in epithelial tissues or develop any pathological and/or metabolic disorders associated with the failure of epithelial organs. Analysis of the tumor spectrum in animals observed for over 2 years did not reveal increased incidence of spontaneous tumors in epithelial organs. No abnormalities were detected in the cellular morphology or the polarization of intestinal epithelial cells. We also assessed the survival of *frk*/*rak*-null mice following radiation-induced intestinal damage and found that *frk*/*rak*-null mice do not have an altered sensitivity to ionizing radiation. Finally, using large-scale cDNA microarray expression analysis, we have identified sets of differentially regulated genes, which led to the discovery of a subtle physiological defect in *frk*/*rak*-null mice resembling euthyroid sick syndrome (ESS).

MATERIALS AND METHODS

Generation of *frk*/*rak*-null mice. Genomic clones for *frk*/*rak* were isolated from a 129 Sv/Ev mouse genomic DNA library, kindly provided by David C. Lee (University of North Carolina—Chapel Hill, Chapel Hill). Libraries were screened with a 1.1-kb murine *frk*/*rak* cDNA probe that encodes the entire open reading frame, except the kinase domain, to avoid cross-reaction with other SFKs. A 13.5-kb genomic clone containing exons 1a and b, which encode the 5′ untranslated region and the N-terminal and SH3 domains, respectively, was used to generate the two flanking arms. The 4.5- and 3.8-kb arms were cloned into the targeting vector pJNS2, kindly provided by Beverly H. Kolller (University of North Carolina—Chapel Hill), on either side of the neomycin phosphotransferase cassette (see Fig. 2A). The linearized targeting vector was electroporated into E14TG2a embryonic stem (ES) cells, and then they were placed under neomycin and ganciclovir selection to obtain 64 resistant clones (34). ES clones were analyzed by Southern blotting with a [^{32}P]dCTP labeled 1.8-kb genomic fragment (see Fig. 2A) and a neomycin cDNA probe to confirm correct targeting. Two of the three targeted ES clones identified were injected into 3.5-day-old C57BL/6J blastocysts and implanted in C57BL/6J pseudopregnant mothers to generate chimeras (34). Chimeras were bred with C57BL/6J males and females (Charles River Laboratories) for germ line transmission of the targeted allele. Transmitting chimeras (males) were also bred to 129 Sv/Ev females (Taconic, Germantown, N.Y.) to establish heterozygotes in the 129 inbred genetic background. Heterozygotes obtained in the 129-BL/6 mixed genetic and 129 inbred backgrounds were intercrossed to generate +/+, +/−, −/− mice. All the analysis described in this report was done with cohorts of mice maintained on the 129-BL/6 mixed genetic background

Genotyping of mice. DNA was isolated from 1-cm-long tail biopsies of weaned mice by using the high-salt precipitation method for Southern blotting (31) or the QIAmp tail DNA isolation kit (Qiagen, Inc.) for PCR screening. For Southern blotting, genomic DNA was digested with *Eco*RV and electrophoresed on 0.8% agarose gels. DNA was transferred to nylon Hybond membranes (Amersham Ltd.) by capillary transfer and cross-linked to the membranes by UV cross-linking in a Stratalinker (Stratagene, La Jolla, Calif.). Membranes were probed with a [^{32}P]dCTP random primer-labeled 1.8-kb *Kpn-Eco*RV genomic fragment (5′ end probe) (see Fig 2A). The primer pairs used for PCR-based genotyping are sense primer iyk 1 (5′-CACCATGGGCAGCGTCTGTGTGAGA-3′) and antisense primer iyk 12 (5′-CGCCACGTAATTGGAAGGAATGTAG-3′), which generate a 343-bp band corresponding to the wild-type allele. The primer pair consisting of sense primer pNeo1 (5′-TGCTCGACGACGTTGTCACT-3′) and antisense primer pNeo3 (5′-TCATCCTGATCGACAAGACC-3′) was used to generate a 196-bp band corresponding to the targeted allele. All PCRs for genotyping were performed with the *Taq* PCR master mix kit (Qiagen Ltd.).

RNA isolation and Northern analysis. The organs of interest were isolated and snap frozen in liquid nitrogen. Total RNA was isolated from frozen organs homogenized in Trizol reagent (GIBCO-BRL Ltd.) according to the manufacturer's protocol. Twenty micrograms of total RNA was electrophoresed on 1.2% formaldehyde–agarose gels and then transferred to Hybond nylon membranes (Amersham Ltd.) by capillary transfer. Blots were probed with [^{32}P]dCTP-labeled full-length murine *frk*/*rak*, *fyn*, and *src* cDNA probes and PCR-amplified murine c-*yes* and glyceraldehyde-3-phosphate dehydrogenase (GAPDH) cDNA probes. Membranes were hybridized in Express Hyb (Clontech) at 68°C overnight, washed in 2× SSC (1× SSC is 0.15 M NaCl plus 0.015 M sodium citrate) and 0.1% sodium dodecyl sulfate (SDS) at room temperature, and washed in 0.1× SSC and 0.1% SDS at 50°C. Membranes were then exposed to XO-MAT-AR (Kodak) autoradiography film. Autoradiographs were scanned, and quantitation of the signal was performed with National Institutes of Health (NIH) IMAGE, version 6.2, software to obtain normalized ratios of expression for SFK genes. The average value of change in SFK gene expression for three *frk*/*rak*-null mice compared to age-matched wild-type controls was calculated.

Western blotting analysis. Total protein from tissues of interest was obtained by homogenization with a tissue homogenizer (Fisher Scientific Ltd.) in lysis buffer (20 mM HEPES, 0.15 M NaCl, 2 mM EDTA, 2 mM EGTA, 1% Triton X-100, 500 μM sodium orthovanadate, 50 μM sodium molybdate, 10 μg of aprotinin/ml, 10 mM sodium fluoride, 10 μg of leupeptin/ml). Lysates were electrophoresed on SDS–10% polyacrylamide gel electrophoresis (PAGE) gels, transferred to polyvinylidene difluoride membranes (Millipore), and probed with polyclonal rabbit antibodies directed against the SH2 and SH3 domains of murine Frk/rak (gift of Michael Welsh, Uppsala University, Uppsala, Sweden). Rabbit polyclonal antibodies directed against beta-casein were used at a 1:500 dilution (gift of Nancy Hynes, Friedrich Meischer Institute, Basel, Switzerland). Sheep anti-rabbit secondary antibodies (Amersham Ltd.) were used at a 1:5,000 dilution and membranes were developed using the enhanced chemiluminescence (ECL) reagent (Amersham Ltd.). Membranes were then exposed to Hyperfilm (Amersham Ltd.) for the detection of the signal.

Histological analysis and electron microscopy. All organs were fixed in 10% normal-buffered formalin overnight; embedded in paraffin and sectioned at 4-micron thickness (American Histolabs, Gaithersburg, Md.). Sections were stained with hematoxylin and eosin. Histological analysis of all tissues was performed by Miriam Anver, National Cancer Institute (NCI), Frederick Cancer Research and Development Center, Frederick, Md. Tissue preparation for electron microscopic ultrastructural studies was performed as described previously (14). Pieces of freshly isolated mouse jejunum were initially fixed in 4% paraformaldehyde and 2% glutaraldehyde in phosphate-buffered saline (pH 7.4). The tissues were postfixed, dehydrated, and embedded in epoxy resin. The cured embedded blocks were sectioned at approximately 50 to 60 nm with the Ultracut microtome (Leica, Bannockburn, Ill.). Thin sections were mounted on a naked copper mesh grid and stained with uranyl acetate and lead citrate solution to enhance the contrast. Sections were examined and photographed with an H7000 electron microscope (Hitachi, Tokyo, Japan) operated at 75 kV. All transmission electron microscopy (TEM) and scanning electron microscopy (SEM) analyses were performed by Kunio Nagashima, NCI, Frederick Cancer Research and Development Center, NIH.

Irradiation of animals for intestinal injury. Cohorts of 9.5- to 11-week-old males and females comprising all three genotypes were obtained by heterozygous intercrosses and housed under normal conditions. Animals were placed in Lucite boxes (five at a time) and exposed to a single dose of 9, 10, 11, or 12 Gy of whole-body gamma-irradiation delivered from a cesium-137 irradiator at a rate of 1 Gy/min. Animals were observed for 10 days and monitored daily for health and mortality. The number of surviving animals of each genotype was recorded on day 10 postirradiation to calculate the $LD_{50/10}$ survival percentages. $LD_{50/10}$ is defined as the dose that results in 50% mortality of animals in 10 days.

Radiation injury and survival experiments were performed in triplicate for the 10- and 11-Gy doses and in duplicate for the 9-Gy dose with 6 to 12 animal cohorts per genotype. The day 10 percent survival per dose represents the average value with standard error for all experiments.

Statistical analysis. All statistical analysis for the radiation survival experiments was kindly performed by Seth M. Steinberg, Biostatistics and Data Management Section, Center for Cancer Research, NCI. The comparisons of the fractions of wild-type, heterozygous, and mutant *frk*/*rak* animals, which did not survive past 10 days, were done with the chi-square test or Fisher's exact test as appropriate. All *P* values indicated are two tailed. The Kaplan-Meir method was used for the calculation of the median survival of mice.

cDNA microarray expression analysis. The organs of interest were isolated from 3- to 4-month-old *frk*/*rak*$^{+/+}$ and *frk*/*rak*$^{-/-}$ littermate males maintained under normal conditions and frozen immediately in liquid nitrogen. Frozen tissues were homogenized in Trizol reagent (GIBCO-BRL Ltd), and total RNA was isolated. In order to control for variability between animals and increase reproducibility, comparisons were performed for four pairs of *frk*/*rak*$^{+/+}$ and *frk*/*rak*$^{-/-}$ littermates and in triplicate for each pair (including a reciprocal experiment). Three micrograms of total RNA was used for RNA amplification performed with the modified method of Phillips and Eberwine (41). Briefly, first-strand cDNA synthesis was performed with Superscript II reverse transcriptase (GIBCO-BRL) and a T7-oligo(dT) primer and second-strand cDNA was synthesized with DNA polymerase I. In vitro transcription to amplify RNA was performed with the T7 Megascript kit (Ambion Ltd.) by following the manufacturer's instructions. Ten micrograms of amplified RNA from each sample (*frk*/*rak*$^{+/+}$ or *frk*/*rak*$^{-/-}$) was reverse transcribed, incorporating either Cy3 or Cy5 dUTP (NEN) nucleotides to generate fluorescently labeled probes. The 2,700 cDNA element mouse expression microarrays used in the experiments described here were printed at the NCI array facility, Advanced Technology Center, NCI, NIH. The Cy3- and Cy5-labeled probes (corresponding to *frk*/*rak*$^{+/+}$ and *frk*/*rak*$^{-/-}$ samples) were mixed together, denatured at 100°C, and applied to the chips in hybridization buffer (25% formamide, 5× SSC, and 0.1% SDS). Microarrays were hybridized overnight at 42°C, washed sequentially in 2× SSC, 0.1% SDS, 1× SSC, 0.1% SDS, 0.2× SSC, and 0.5× SSC, air dried, and scanned at wavelengths corresponding to the two fluorochromes with a Genepix 400A microarray scanner (Axon Instruments, Union City, Calif.). The intensities of the Cy3 and Cy5 signals for every feature on the array were recorded, and normalized signal ratios (after background subtraction) were obtained for each element with the GenePix Pro 3.0 microarray analysis software (Axon Instruments). The complete data set for each array was deposited into the NCI microarray database, maintained by the Center for Information Technology, NCI, NIH. All genes that displayed a concordant change in expression of 1.2-fold (baseline changes) or more and, conversely, of 0.8-fold and below (calculated as the normalized ratio of expression in *frk*/*rak*$^{-/-}$ to *frk*/*rak*$^{+/+}$) in at least two of the three pairwise comparisons per animal pair were selected to generate a primary list of potential Frk/rak-responsive candidates. The primary database of all potential candidates was analyzed to identify genes that consistently displayed a change in expression of 1.5-fold or more in at least three out of four *frk*/*rak*$^{-/-}$ animals. All higher level analysis, such as comparison of expression patterns of genes in multiple arrays or over multiple tissues and organs, was performed with web-based multiarray analytical tools available and custom bioinformatics tools developed in the laboratory.

Measurement of thyroid hormone levels. Two- and 3-month-old *frk*/*rak*$^{+/+}$ and *frk*/*rak*$^{-/-}$ littermates were starved overnight, and whole blood was collected by cardiac puncture. Blood was allowed to clot at room temperature for at least 1 h, and serum was collected after centrifugation at 10,000 × *g* for 10 min at 4°C. The total circulating levels of the thyroid hormones T3, T4, and thyrotropin (TSH) (free and bound fractions) were quantitated by enzyme-linked immunoassay (AniLytics, Inc., Gaithersburg, Md.). To assess statistical significance, a Wilcoxon signed rank test was performed on the sibling-paired difference between the log values of total circulating levels of T3 (and T4) in *frk*/*rak*$^{+/+}$ and matched *frk*/*rak*-null littermates. Statistical analysis was kindly performed by Dominic T. Moore at the Biostatistics Shared Resources Group, Lineberger Comprehensive Cancer Center, University of North Carolina—Chapel Hill.

RESULTS

Analysis of Frk/rak expression in mouse tissues. Previous studies indicate that *frk*/*rak* expression is restricted to tissues of epithelial origin. To extend these studies and identify tissues that are likely to be affected by loss of *frk*/*rak*, we examined Frk/rak protein expression in a panel of adult tissues. The highest levels of Frk/rak protein were detected in the gastrointestinal tract and the pancreas. Frk/rak could also be easily detected, albeit at lower levels, in the kidney, ovary, lung, and liver. Levels of Frk/rak were extremely low in the whole brain, virgin breast, and spleen, and no Frk/rak could be detected in the heart (Fig. 1A). While Frk/rak is barely detectable in the prepubescent and resting virgin mammary gland, Frk/rak protein levels increase during pregnancy (Fig. 1B and C), with expression peaking at day 16 of pregnancy. Maximal Frk/rak expression is detected after 24 h of involution, and levels return to those detected in the virgin and resting gland by day 5 of involution.

Analysis of *frk*/*rak*-null mice. We designed a targeting construct that, upon homologous recombination with the wild-type *frk*/*rak* allele, results in replacement of exons 1a and b with the neomycin gene. As exon 1b encodes the 5′ untranslated region, the translation initiation codon, N-terminal sequences, and the complete SH4 and SH3 domains of Frk/rak, we expected that this recombination event would generate a null *frk*/*rak* allele (Fig. 2A). Mouse lines were derived from two ES cell clones carrying the *frk*/*rak*-null allele. No differences were detected in the phenotypes of these two lines. Heterozygous males and females exhibited no obvious abnormalities. *frk*/*rak*$^{-/-}$ pups were obtained at the expected Mendelian ratio in litters obtained from heterozygous intercrosses of mice both on the mixed and 129 genetic backgrounds (Table 1). Northern analysis of total RNA derived from the kidney, small intestine, and colon of *frk*/*rak*$^{-/-}$ mice failed to detect any of the three transcripts encoding Frk/rak (Fig. 2C). Similarly, Western analysis revealed the absence of Frk/rak protein in tissues derived from *frk*/*rak*$^{-/-}$ mice (Fig. 2D). Loss of *frk*/*rak* did not affect neonatal development, as *frk*/*rak*$^{-/-}$ pups could not be distinguished from their wild-type littermates by differences in size or appearance. No obvious changes in cage exploration, social behavior, or response to stimuli were observed in *frk*/*rak*$^{-/-}$ mice. *frk*/*rak*$^{-/-}$ adult males and females were fertile and yielded litters of sizes comparable to those generated by wild-type mice after mating to C57BL/6J animals. Additionally *frk*/*rak*$^{-/-}$ females were able to bear and sustain litters as efficiently as their wild-type and heterozygous littermates. Comparisons of *frk*/*rak*-null and control animals did not reveal any obvious changes in size or growth from weaning to 12 months of age. Age-matched 2-, 5-, 8-, and 12-month-old *frk*/*rak*$^{+/+}$ and *frk*/*rak*$^{-/-}$ littermates from the F_2 generation were euthanized, and a complete (greater than 20 organs) histopathological analysis was performed. No differences were observed between the three different groups in the number or types of lesions present in various organs (data not shown). A nearly 200-animal cohort (F_2 generation) consisting of +/+, +/−, and −/− animals was monitored for health and mortality up to 28 months of age. No significant increase in the incidence of any pathological lesions, including spontaneous tumors, was detected in *frk*/*rak*$^{-/-}$ animals (data not shown).

Analysis of the ultrastructure of the intestinal epithelium in *frk*/*rak*-null mice. The rat homolog of Frk/rak has been reported to localize to the apical membranes (brush borders) of intestinal enterocytes. Expression levels and subcellular localization of Frk/rak correlated with cytodifferentiation of the intestinal epithelium. Furthermore, Frk/rak has been re-

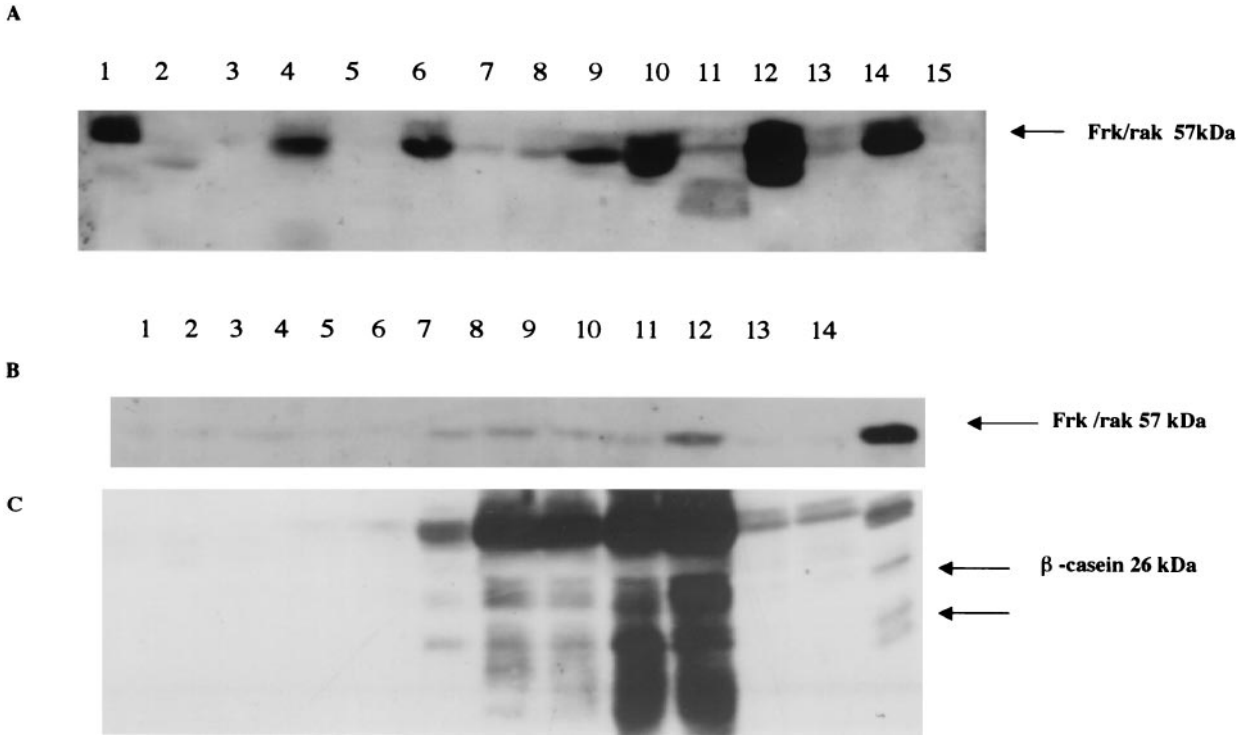

FIG. 1. Expression of Frk/rak in adult murine tissues. Total protein was isolated from a panel of organs derived from 2-month-old male and female C57BL/6J mice (Charles River Laboratories). Two hundred micrograms of total protein was electrophoresed on SDS–10% PAGE gels. (A) Western blots were probed with anti-Frk antibodies used at a 1:500 dilution (Michael Welsh, Uppsala University) and then with donkey anti-rabbit horseradish peroxidase-conjugated secondary antibody (Amersham) used at a 1:5,000 dilution. Blots were developed with ECL reagent (Amersham). Mouse Frk/rak is detected as a 57-kDa band. Lane 1, 50 μg of NmuLi cell lysate control; lane 2, brain; lane 3, breast; lane 4, colon; lane 5, heart; lane 6, kidney; lane 7, liver; lane 8, lung; lane 9, ovary; lane 10, pancreas; lane 11, skeletal muscle; lane 12, small intestine; lane 13, spleen; lane 14, stomach; lane 15, testis. (B) Expression of Frk/rak protein increases during normal murine mammary gland differentiation. Murine mammary glands were isolated at different time points during the developmental cycle of healthy C57BL/6J female mice. Tissues were homogenized, 200 μg of total protein was electrophoresed on SDS–10% PAGE gels, and transferred to Immobilon-P (Millipore) membranes. Blots were incubated with primary Bsk-specific polyclonal antibodies used at a 1:500 dilution (Michael Welsh, Uppsala University) and with donkey anti-rabbit horseradish peroxidase-conjugated secondary antibody (Amersham) used at a 1:5,000 dilution. Blots were developed with ECL reagent (Amersham). Top panel lanes: 1, 4-week-old virgin; 2, 6-week-old virgin; 3, 10-week-old virgin; 4, day 6 of pregnancy; 5, day 9 of pregnancy; 6, day 14 of pregnancy; 7, day 16 of pregnancy; 8, day 3 of lactation; 9, day 8 of lactation; 10, day 1 of involution; 11, day 5 of involution; 12, day 10 of involution; 13, 50-μg NmuLi cell lysate (control for Frk/rak). For the results shown in the bottom panel, lysates were probed with rabbit polyclonal antibodies directed against beta-casein used at a 1:1,000 dilution (Nancy Hynes, Friedrich Meischer Institute) Lanes 1 to 12, same as for top panel; lane 13, 100-μg lysate of HC11 cells induced to differentiate for 10 days with prolactin (control for beta-casein antibody).

ported to colocalize with c-met in the brush borders of rat intestinal enterocytes. Frk/rak activity increased in response to hepatocyte growth factor (HGF) stimulation in vitro (17), suggesting that Frk/rak is downstream of the HGF receptor and could potentially participate in epithelial morphogenic programs mediated by HGF signaling. We therefore initiated a detailed investigation of the morphology of the intestinal mucosa. Histological analysis of sections of the small intestine derived at different ages from age-matched *frk/rak*$^{+/+}$ and *frk/rak*$^{-/-}$ littermates did not reveal any difference in the morphology of the epithelium. To determine if the ultrastructure of intestinal enterocytes and their apical membranes was altered in *frk/rak*-null mice, SEM and TEM were performed on sections of the jejunum. The apico-basal polarity of the enterocytes was found to be structurally intact, as ascertained by proper intracellular positioning of organelles like the nucleus and Golgi apparatus (Fig. 3A). No significant differences were observed in the length, diameter, arrangement, and packing of the microvilli in the brush border (Fig. 3B). Frk/rak protein (endogenous and ectopically expressed) has been localized to the Golgi and centrosomal compartments in a number of cell lines. TEM analysis also failed to reveal any abnormalities in either the intracellular localization or the ultrastructure of centrioles in *frk/rak*$^{-/-}$ enterocytes (Fig. 3C and D).

TABLE 1. Genotypic analysis of offspring from heterozygous intercrosses

Genetic background	Gender group	No. (%) of genotype:		
		+/+	+/−	−/−
129-BL/6	Male	37 (26.8)	71 (51.4)	30 (21.7)
	Female	37 (25.7)	66 (45.8)	41 (28.5)
	Combined	74 (26.2)	137 (48.6)	71 (25.2)
129ola × 129SvEv	Male	12 (26.1)	22 (47.8)	12 (26.1)
	Female	9 (26.5)	16 (47.1)	9 (26.5)
	Combined	21 (26.3)	38 (47.5)	21 (26.3)

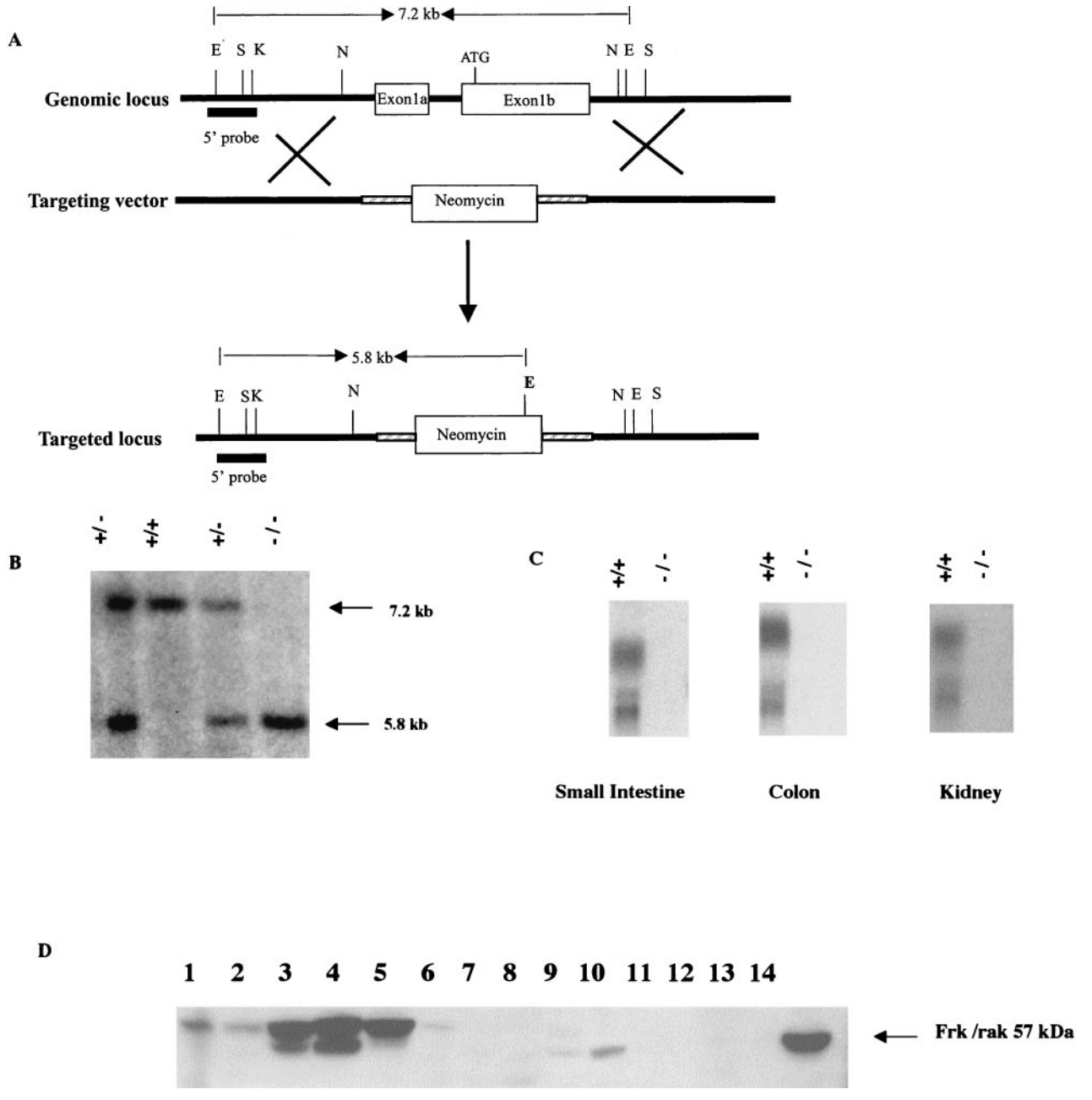

FIG. 2. Scheme for generation of a targeted disruption in *frk*/*rak*. (A) A targeting construct was generated such that homologous recombination would result in the replacement of exons 1a and b with the neomycin phosphotransferase selection marker cassette. This design results in the removal of the first methionine and the translation initiation site of the protein, indicated ATG. The replacement of exons 1a and b with the neomycin cassette also results in the introduction of a novel *Eco*RV site as shown (bold E). Sites for restriction enzymes are shown as follows: E, *Eco*RV; S, *Sal*I; K, *Kpn*I; N, *Nhe*I. The 5′ probe, a 1.8-kb *Kpn*I-*Eco*RV fragment, thus detects a 5.8-kb fragment from the mutant allele compared to a 7.2-kb fragment detected from the wild-type allele (untargeted) in *Eco*RV-digested genomic DNA. (B) Representative Southern blot of mice generated by heterozygous crosses. Tail DNA was digested with *Eco*RV, and Southern blots were probed with the 5′ probe. Wild-type, heterozygous, and homozygous mutant mice are identified based on the presence of the 7.2-kb (wild type) and 5.8-kb (mutant) *Eco*RV bands. The disruption introduced in *frk*/*rak* produces a null mutation. (C) Northern blot analysis was performed on total RNA derived from the small intestine, colon, and kidney of 4-month-old age-matched littermates. Twenty micrograms of total RNA was electrophoresed on 1.2% formaldehyde–agarose gels. Northern blots were probed with [^{32}P]dCTP-labeled *frk*/*rak* complete cDNA. (D) Western blot analysis was performed on total protein isolated from organs derived from age-matched littermates. Two hundred micrograms of the total cellular protein isolated was analyzed with polyclonal murine anti-Frk antibodies. Lanes 1 to 6, *frk*/*rak*$^{+/+}$ mice; lanes 7 to 12, *frk*/*rak*$^{-/-}$ mice; lanes 1 and 7, liver; lanes 2 and 8, lung; lanes 3 and 9, kidney; lanes 4 and 10, stomach; lanes 5 and 11, colon; lanes 6 and 12, spleen; lane 14, NmuLi cell lysate (control for murine anti-Frk antibody).

Histological analysis of other organs, such as the kidney and lung, which contain polarized epithelia and brush borders, also did not reveal any morphological defects (data not shown). In addition, despite high levels of expression in the differentiating mammary gland, female *frk*/*rak*$^{-/-}$ mice successfully nursed litters, and normal branching and alveolar differentiation was detected in their mammary glands (data not shown).

Survival of *frk*/*rak*-null mice after radiation-induced intestinal injury. Intestinal epithelial cells are extremely sensitive to ionizing radiation, and the loss of epithelial integrity primarily contributes to the death of animals within 10 days of exposure to 10- to 12-Gy doses of whole-body radiation. A functional role for Frk/rak in epithelial cell death, damage repair, and/or proliferation and differentiation might alter the radiation sensitivity and survival of *frk*/*rak*$^{-/-}$ mice following acute injury. To address this, age-matched (9.5 to 11 week old) cohorts of mice consisting of *frk*/*rak*$^{+/+}$, *frk*/*rak*$^{+/-}$, and *frk*/*rak*$^{-/-}$ mice were exposed to a single dose of 9, 10, 11, or 12 Gy of whole-body ionizing radiation, and the percent survival of each genotype was determined on day 10 postirradiation. Exposure to 12 Gy caused complete mortality of all genotypes before day 10 (data not shown). At 11 Gy, approximately 50% survival was observed in the control groups (+/+ and +/− mice) The $LD_{50/10}$ survival of *frk*/*rak*$^{-/-}$ mice did not differ significantly from that of the *frk*/*rak*$^{+/+}$ (59.5% ± 13.4% versus 52.2% ± 27.7%, $P = 0.68$) and *frk*/*rak*$^{+/-}$ (59.5% ± 13.4% versus 53% ± 18.3%, $P = 0.84$) animals (Table 2). The survival of all three groups increased after exposure to 10 and 9 Gy of radiation, and no significant differences were observed in the day 10 percentage survival of *frk*/*rak*$^{-/-}$ mice compared to the control groups at both of these doses (Table 2). The median survival of *frk*/*rak*-null mice over 2 weeks following exposure to 10 Gy also did not differ significantly from that of the control groups (Table 3). Furthermore, qualitative histological analysis of apoptosis and mitosis performed on sections of the jejunum isolated from *frk*/*rak*$^{-/-}$ mice 1, 3, 7, and 10 days after exposure to 10 Gy revealed no significant differences in the morphology of the regenerating intestinal epithelium compared to that of the controls (data not shown).

Expression analysis of SFK genes in *frk*/*rak*-null mice. The failure of Frk/rak disruption to result in defects in growth and morphology of intestinal epithelial cells could be the consequence of compensatory changes in the expression of SFK genes or other cellular pathways. To examine this possibility, we compared the global gene expression profiles in various organs of *frk*/*rak*$^{-/-}$ and *frk*/*rak*$^{+/+}$ mice by using cDNA microarrays. While the majority of changes were in the range of 1.2-fold, alterations in the expression (even as low as 1.5-fold) of certain genes were consistently detected in multiple tissues of *frk*/*rak*-null mice (data not shown). The mouse cDNA arrays used in the analysis included SFKs (*src*, *fyn*, *yes*) and members of the Frk/rak family (*sik*). Interestingly, a 2.2- and 2.1-fold increase in c-*src* expression was detected in the intestine and kidney, respectively, of *frk*/*rak*$^{-/-}$ mice (Fig 4A). Additionally, a modest (1.38-fold) increase in *yes* expression was detected in the colon of *frk*/*rak*-deficient mice. To verify these findings, Northern blot analysis of the expression of SFKs, *src*, *fyn*, and *yes* was performed with total RNA isolated from the colon, kidney, and jejunum of *frk*/*rak*$^{+/+}$ and *frk*/*rak*$^{-/-}$ mice. While expression of c-*src* increased by 1.9-fold in the intestine and 1.4-fold in the colon (Fig. 4 B), no changes in the expression of *yes* and *fyn* were detected in either organ (data not shown).

Investigation of the thyroid hormone status of *frk*/*rak*-null mice cDNA expression analysis provides clues to biochemical phenotypes. An analysis of all genes identified with a differential expression of 1.2-fold or more in *frk*/*rak*$^{-/-}$ animals surprisingly revealed a subset of genes in common to those identified by microarray expression analysis of rat pituitary cells treated with T3 hormone in vitro (43). A qualitative comparison was therefore performed between all genes differentially expressed in *frk*/*rak*$^{-/-}$ mice and in a panel of organs isolated from mice injected with T3 hormone (L. D. Miller, unpublished data). Consistent with our earlier observation, genes identified in *frk*/*rak*-null mice were also represented in this set of T3-responsive candidates, which included genes and gene families regulated at the transcriptional level by thyroid hormones and those associated with T3 signaling. This finding presented the intriguing possibility that thyroid hormone levels or signaling may be altered in *frk*/*rak*-null mice. Circulating levels of T3, T4, and TSH were therefore measured for 10 pairs of age-matched *frk*/*rak*$^{+/+}$ and *frk*/*rak*$^{-/-}$ littermates. Total circulating levels of T3 were decreased in 80% (8 out of 10 pairs, $P = 0.019$) of *frk*/*rak*$^{-/-}$ animals compared to their *frk*/*rak*$^{+/+}$ littermates (Fig. 5A). However, no significant changes were detected in the circulating levels of T4 ($P = 0.84$) (Fig. 5B) and TSH (data not shown).

DISCUSSION

This study clearly demonstrates that *frk*/*rak* is not essential for embryonic development, as viable *frk*/*rak*-null mice are obtained at the predicted Mendelian frequency in different genetic backgrounds. Furthermore, histopathological analysis of over 20 organs derived from age-matched *frk*/*rak*-null and wild-type littermates, failed to identify any deficits in the development of epithelial tissues that normally express high levels of this kinase. Also, no overt defects in the physiological functions of all major organs were identified, as illustrated by the good health and normal growth of *frk*/*rak*$^{-/-}$ animals. Human *frk*/*rak* localizes to chromosome 6q21-23, and the

TABLE 2. Comparison of survival of *frk*/*rak*-null mice after exposure to single doses of ionizing radiation[a]

Dose (Gy)	% Survival ± SEM on day 10 (*n*) of genotype:			Statistical significance
	+/+	+/−	−/−	
11	52.2 ± 27.2 (13)	53 ± 18.4 (31)	59.5 ± 13.4 (23)	0.80[b] 0.84[c] 0.68[d]
10	82.3 ± 16.6 (25)	78.7 ± 11.2 (37)	69.9 ± 21.2 (31)	0.75[b] 0.69[c] 0.37[d]
9	100 (21)	100 (25)	87.5 ± 2.2 (25)	N/A[b,e] 0.24[c] 0.23[d]

[a] Data is cumulative from two separate trials (9 and 11 Gy) and three separate trials (10 Gy). Cohorts consist of 9.5- to 11-week-old age-matched littermates generated by heterozygous intercrosses with nearly 50% male and females.
[b] *P* value for +/+ versus +/− mice is given.
[c] *P* value for +/− versus −/− mice is given.
[d] *P* value for +/+ versus −/− mice is given.
[e] N/A, not applicable.

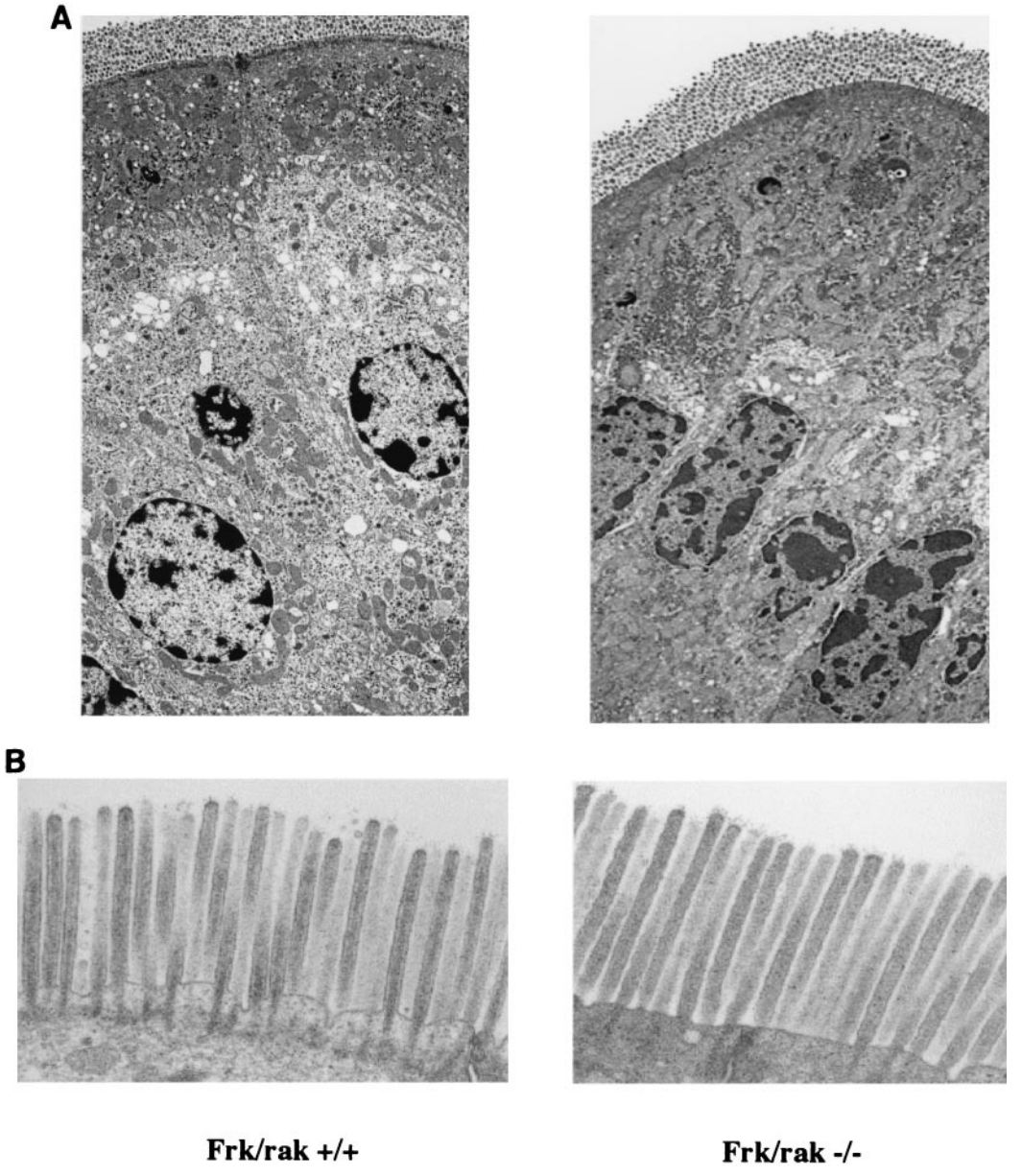

FIG. 3. Morphological analysis of intestinal epithelium. *frk*/*rak*$^{-/-}$ enterocytes have normal structural polarization. TEM analysis was performed on ultrathin sections of jejunum derived from age-matched *frk*/*rak*$^{+/+}$ and *frk*/*rak*$^{-/-}$ littermates. (A) As revealed by the low-magnification analysis shown above, *frk*/*rak*$^{-/-}$ enterocytes from the villus maintain normal apico-basal polarity, as defined by the intracellular positioning of organelles like the nucleus and Golgi apparatus. (B) TEM analysis of the brush borders of *frk*/*rak*$^{-/-}$ mice. Sections of the jejunum isolated from 3- to 4-month-old *frk*/*rak*$^{+/+}$ and *frk*/*rak*$^{-/-}$ littermates were fixed appropriately for TEM. Ultrathin sections were cut and analyzed at high resolution to determine the structural integrity, organization, and dimensions of the microvilli that constitute the brush border. TEM analysis reveals normal ultrastructure and dimensions of microvilli in *frk*/*rak*$^{-/-}$ enterocytes compared to that of their wild-type littermates. For *frk*/*rak*$^{+/+}$ mice, the average length is 1.6 μm and the average width is 0.1 μm. For *Frk*/*rak*$^{-/-}$ mice, the average length is 1.6 μm and the average width is 0.1 μm. (C) Subcellular positioning of centrioles in *frk*/*rak*$^{-/-}$ enterocytes. Ultrathin sections of jejunum obtained from age-matched *frk*/*rak*$^{+/+}$ and *frk*/*rak*$^{-/-}$ littermates were analyzed by TEM to determine the position and morphology of centrioles. A representative section from an *frk*/*rak*$^{-/-}$ enterocyte demonstrating characteristic apical localization of centrioles (closer to the plasma membrane) is shown. (D) Centriole structure in *frk*/*rak*$^{-/-}$ mice enterocytes. Ultrathin sections were analyzed by TEM to verify the ultrastructure of the centrioles. The panel shows normal centriolar structure in *frk*/*rak*$^{-/-}$ mice compared to that of *frk*/*rak*$^{+/+}$ mice, as seen by the arrangement of microtubule triplets.

mouse gene *iyk* localizes to the syntenic region on proximal mouse chromosome 10. The 6q21-23 region has been identified as a tumor suppressor and/or senescence locus (35, 43). Taken in conjunction with the finding that overexpression of Frk/rak causes a potent growth arrest in vitro both in human and in murine systems, it was hypothesized that the loss of *frk*/*rak* would lead to epithelial hyperplasias or neoplasias. However, to date (animals observed for greater than 2 years), no spontaneous primary tumors have been observed in the colon, small intestine, kidney, pancreas, and mammary gland

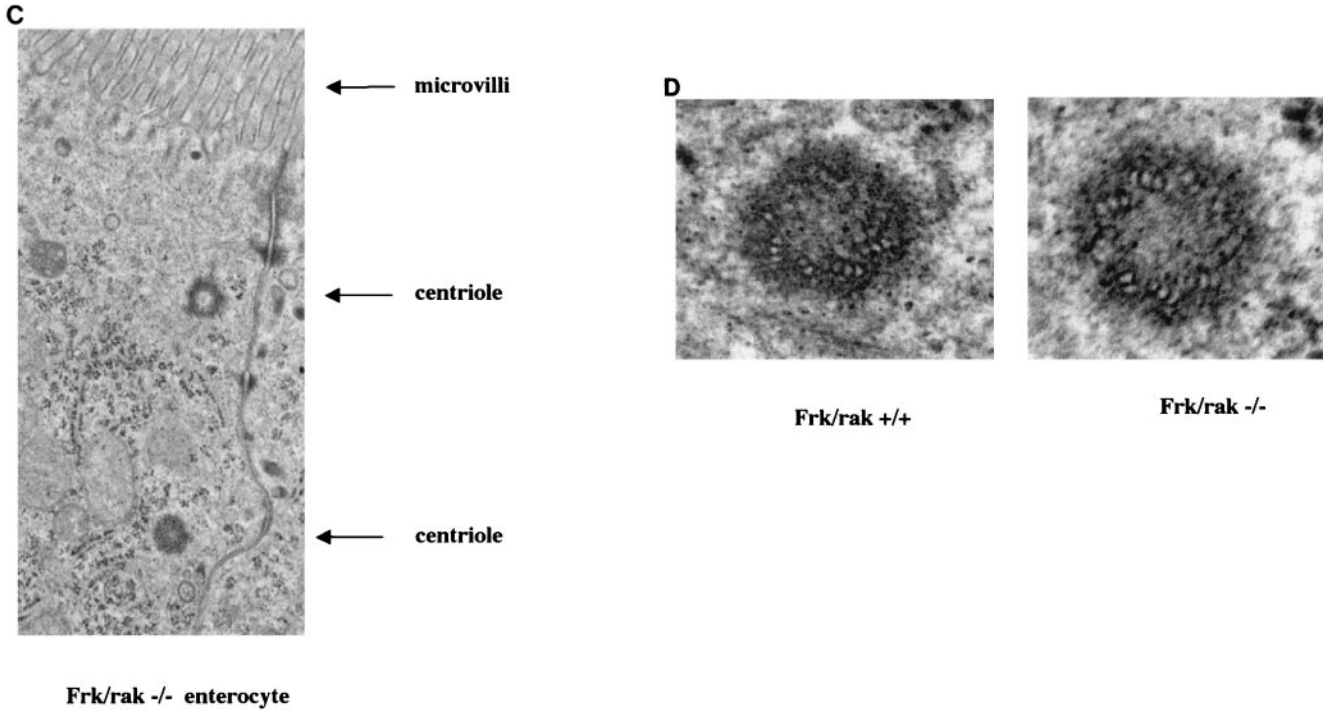

FIG. 3—*Continued.*

of *frk/rak*-null mice. Our studies therefore fail to support a tumor suppressor role for *frk/rak* in the development of epithelial cancers.

Expression studies performed in the developing rat intestine demonstrate that *frk/rak* is detected at low levels in the cytoplasm of the undifferentiated and rapidly dividing intestinal epithelium. Expression levels of the protein increase concomitant with the onset of polarization and formation of early microvilli in the intestinal epithelium. In the adult rat, Frk/rak is detected abundantly in the brush borders of the intestines and at lower levels in the brush borders of polarized epithelial cells in the kidney and lung (16). It was hence speculated that Frk/rak has a functional role in epithelial cytodifferentiation. Histological analysis of adult intestinal tissue derived from *frk/rak*-null mice revealed normal morphological differentiation of the epithelium. The ultrastructure of *frk/rak*$^{-/-}$ enterocytes is normal, and the appropriate subcellular localization of organelles indicates that the apical-basal polarity of cells is intact. The normal dimensions and packing of microvilli revealed by TEM and SEM experiments further indicate that *frk/rak* is not essential for determining or maintaining the structural integrity of the brush border.

TABLE 3. Comparison of median survival of *frk/rak*-null mice over 14 days after exposure to 10 Gy of radiation[a]

Dose (Gy)	Median survival in days for genotype:			Statistical significance
	+/+	+/−	−/−	
10	10.7	10.7	10.9	>0.50[b] >0.50[c] >0.50[d] 0.99[e]

[a] Data is cumulative from two separate trials. Cohorts consist of 9.5- to 11-week-old age-matched littermates generated by heterozygous intercrosses.
[b] *P* value for +/+ versus +/− mice is given.
[c] *P* value for +/− versus −/− mice is given.
[d] *P* value for +/+ versus −/− mice is given.
[e] *P* value for +/+ and +/− versus −/− mice is given.

Frk/rak protein has been localized to the Golgi apparatus and centrosomes (Carter et al., unpublished data). The centrosomal localization of Frk/rak is microtubule independent and cell cycle regulated, suggesting that it is a resident centrosomal protein with a potential role in cell cycle regulation. Centrioles of murine intestinal enterocytes are positioned apically, within 1 to 3 μm of the brush border, and the spatial uncoupling of the centrosome from the Golgi apparatus is integral to enterocyte differentiation (21, 22). Using TEM, we have demonstrated that centrioles are apically localized in intestinal *frk/rak*$^{-/-}$ enterocytes and that their ultrastructure is also normal. Our studies thus demonstrate that Frk/rak is not an essential structural component of centrosomes. However, we cannot yet exclude the possibility that minor defects in some aspect of centriolar function may exist in *frk/rak*$^{-/-}$ cells.

To test whether Frk/rak had a role in intestinal regeneration, as suggested by its differential expression along the length of the crypt-villus axis, we exposed *frk/rak*-null mice to a range of doses of whole-body radiation that cause acute intestinal damage. Radiation-induced injury and readaptation have been extensively characterized (15, 28a). Doses of 9 Gy and above result in lethality within 10 days of exposure due to severe gastrointestinal toxicity. Response to intestinal injury involves an immediate wave of apoptosis to overcome DNA damage

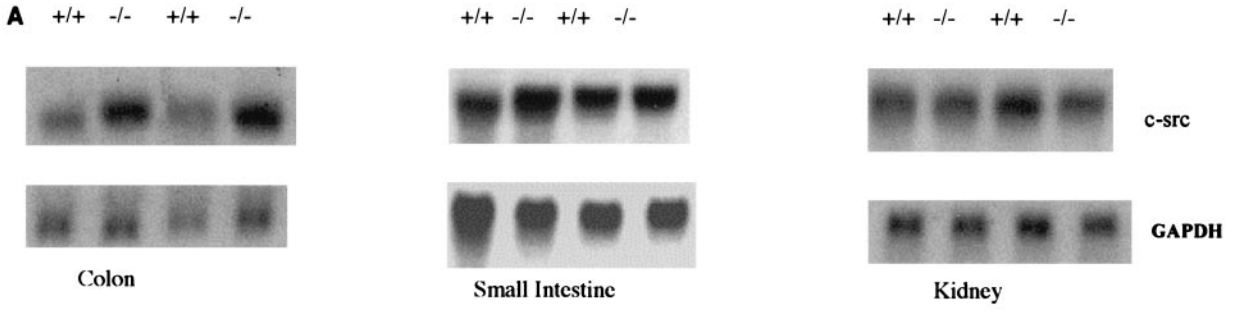

B

Gene	Colon		Intestine		Kidney	
	Northern*	Microarray#	Northern*	Microarray#	Northern*	Microarray#
c-src	1.4	1.0	1.99	2.12	1.0	2.2
c-yes	1.0	1.38	1.0	1.0	1.0	1.0
c-fyn	1.0	1.0	1.0	1.0	1.0	1.0

FIG. 4. Expression of c-*src* in organs of *frk*/*rak*-null mice. (A) The expression of c-*src* was compared in the colon, intestine, and kidney of three pairs of age-matched *frk*/*rak*$^{+/+}$ and *frk*/*rak*$^{-/-}$ littermates. Twenty micrograms of total RNA for each sample was electrophoresed on 1.2% formaldehyde–agarose gels. Northern blots were probed with a full-length mouse c-*src* cDNA probe (provided by Philip Soriano) and with murine GAPDH cDNA (bottom panels) for normalization. (B) Comparison of changes in SFK gene expression by microarray and Northern blot analysis. The normalized ratios of change in gene expression for c-*src* in the intestine, colon, and kidney of *frk*/*rak*-null animals is shown as detected by Northern blotting and microarray analysis separately. Similar analyses were performed for c-*fyn* and c-*yes* with Northern blotting and microarray analysis. A ratio of 1.0 indicates equivalent gene expression in wild-type and null animals. *, increase (*n*-fold) in gene expression in *frk*/*rak*$^{-/-}$ mice (GAPDH-normalized ratios averaged over three pairs); #, increase (*n*-fold) in gene expression in *frk*/*rak*$^{-/-}$ mice (background-normalized ratios averaged for three out of four pairs analyzed).

followed by proliferation and differentiation of the enterocytes to reconstitute the epithelium. A defect in any of these cellular processes would result in altered sensitivity to ionizing radiation, consequently altering the survival of the animals. For example, *Ku80*$^{-/-}$ mice display extreme hypersensitivity to low doses of ionizing radiation, exhibiting complete mortality within 2 weeks of exposure compared to their wild-type counterparts (36). Similarly, PARP$^{-/-}$ mice and mice bearing the *scid* mutation are exquisitely sensitive to gamma-irradiation radiation-induced damage (4, 52). Our study clearly demonstrates that *frk*/*rak*$^{-/-}$ mice do not show significant differences in percent or median survival compared to the control groups, particularly at the $LD_{50/10}$ dosage of 11Gy. We therefore infer that the biological processes responsible for DNA damage repair (apoptosis and cell cycle checkpoints) and regeneration of the intestinal epithelium are not impaired in these animals. It is, however, possible that the *frk*/*rak*-null mutation, in combination with deficiencies in other SFK and Frk genes, which are highly expressed in the colon and intestine, would result in altered radiation sensitivity. Also, loss of *frk*/*rak* may elicit a different response in other models of intestinal injury, such as 5-fluorouracil- or indomethacin-mediated gut toxicity.

The advent of cDNA expression arrays has facilitated broader phenotypical analysis of mouse models with targeted gene disruptions. We performed comparative gene expression profiling of *frk*/*rak*-null and wild-type mice in order to identify molecular phenotypes, which could provide a first approximation of cellular or physiological states, detect potential compensatory mechanisms, and/or provide clues to phenotypes which may become apparent after specific stresses. While the absolute values of severalfold changes in gene expression detected were not dramatic (the majority of genes with a 1.2- to 2.0-fold change), the consistency in the pattern of change across multiple pairwise comparisons strongly suggests that some candidates may indeed represent real responses to *frk* disruption. Interestingly, the number of differentially expressed genes identified in each tissue also correlated with the level of endogenous *frk*/*rak* expression, with the greatest number of outliers detected in the intestine and the least number dectected in the heart (data not shown).

A possible explanation for the lack of an overt defect in *frk*/*rak*-deficient mice is that its functions may be redundant or overlap with those of other members of the Frk/rak and Src families. This does not come completely as a surprise, especially since SFKs have been demonstrated to have redundant functions both in vitro and in vivo. Over the last decade mouse models have been generated with targeted disruptions in all 8 prototypical SFKs. Although in vitro experimentation has associated these versatile proteins with a multitude of biological processes (1, 49), analysis of mice deficient in SFKs reveals

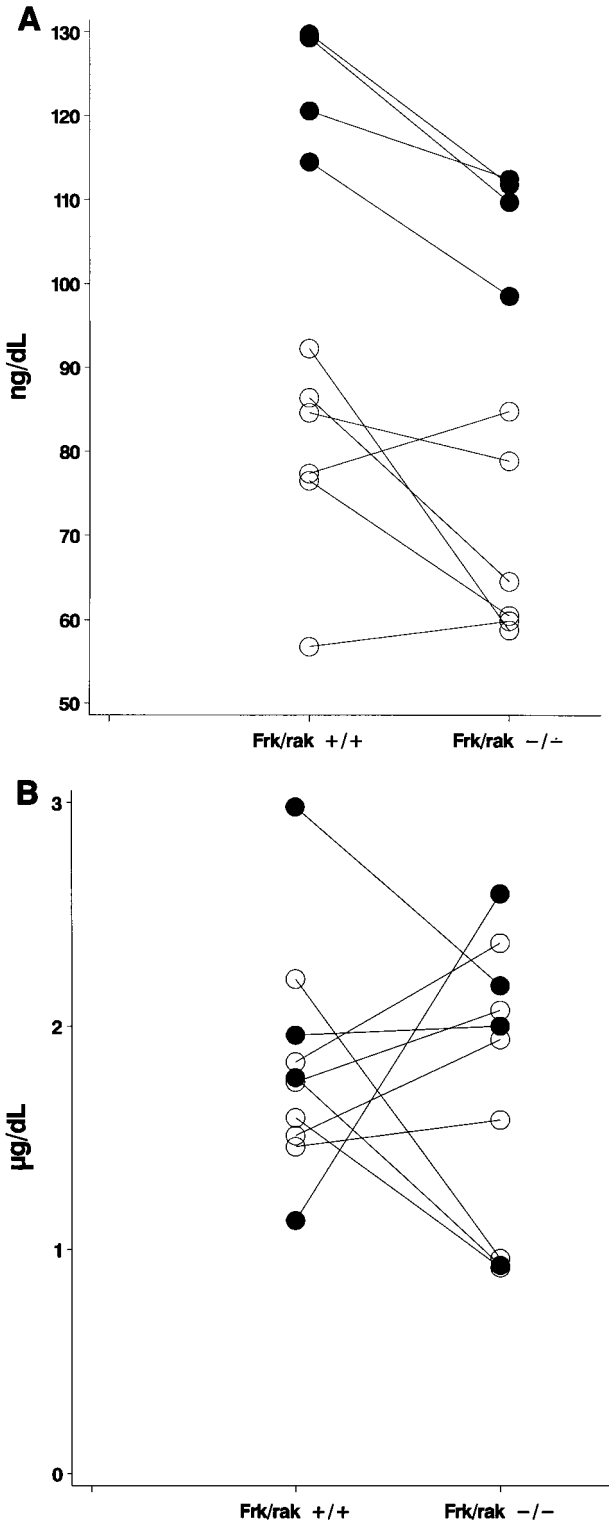

FIG. 5. *frk/rak*-null mice have decreased circulating levels of T3 hormone. A scatter plot analysis of total circulating levels of T3 (A) and T4 (B) hormones in serum obtained from age-matched *frk/rak*$^{+/+}$ and *frk/rak*$^{-/-}$ littermates derived by heterozygous intercrosses. Levels of T3 and T4 hormone in serum were assayed by AniLytics, Inc., as described in Materials and Methods. Comparisons were performed between both male and female littermates of each genotype. *n* (total) = 10; *n* (12-week-old mice) = 4 (●); *n* (8-week-old mice) = 6 (○). Connector lines indicate the actual pairing of *frk/rak*$^{+/+}$ and *frk/rak*$^{-/-}$ littermates.

lesions in restricted cell types and defects in specific cellular processes, as exemplified by the *src*- and *fyn*-null mice (12, 28, 44). A high level of functional redundancy between SFK genes is supported by evidence of compensatory changes in expression, activity, and subcellular localization of other SFKs in mice bearing single mutations, possibly accounting for the minimal phenotypes observed (28, 48). The fact that mice with deficiencies in multiple SFK genes often develop more-severe phenotypes or novel and complex phenotypes not observed in the single mutants is also consistent with this. For instance, expression and activity of hck is elevated in *src*$^{-/-}$ osteoclasts and *src*$^{-/-}$ *hck*$^{-/-}$ mice develop a more-severe osteopetrosis phenotype (27). Another example pertinent to our study is that *fyn*$^{-/-}$ mice have minor phenotypes, and *yes*$^{-/-}$ mice have no overt defects. The *fyn*$^{-/-}$ *yes*$^{-/-}$ mice, however, exhibit increased perinatal lethality, and viable double-null animals develop severe glomerulonephritis (46).

Interestingly, the intestine and colon, which are physiologically similar, express the highest endogenous levels of *frk/rak* as well as high levels of *sik*, c-*src* and c-*yes*. An approximately 2.0-fold increase in the expression of c-*src* detected in *frk/rak*$^{-/-}$ intestines by cDNA microarray and Northern blot analysis suggests a compensatory role for c-*src* in the intestine. Elevated expression of c-*src* mRNA (1.4-fold) is also detected in *frk/rak*$^{-/-}$ colon tissue, further supporting this hypothesis. Although Src and frk/rak may have distinct subcellular localizations, c-*src* could potentially compensate for *frk/rak* by participating in the same or a complementary signaling pathway through interactions with common downstream elements. While no changes in the expression of *sik* were detected in our analysis, it remains possible that changes in Sik levels or activity may compensate for loss of *frk/rak* function.

The observation that some of the differentially expressed genes identified by microarray analysis also appear as potential T3 hormone-responsive genes presented the intriguing possibility that the thyroid hormone status of *frk/rak*-deficient mice may be altered. These included novel candidates and others reported to be transcriptionally regulated by thyroid hormones such as IGFII, ferritin, and peptidyl-alpha-amidating-monooxygenase (PAM) (30). Elevated expression of PAM RNA has been demonstrated in hypothyroid and euthyroid rats (40). An increase in PAM gene expression was detected in the intestine, colon, and kidney of *frk/rak*-null mice, suggestive of a hypothyroid state (data not shown). Similarly, decreased expression of ferritin detected in *frk/rak*$^{-/-}$ intestines was consistent with a defect in T3 hormone-dependent transcriptional regulation (18; data not shown). Quantitative measurements of circulating levels of thyroid hormones indeed revealed a statistically significant ($P = 0.019$) decrease in T3 levels of *frk/rak*$^{-/-}$ animals but no significant changes in the circulating levels of T4 or TSH compared to their age-matched wild-type littermates. The circulating thyroid hormone profile observed in *frk/rak*-deficient mice is reminiscent of that described for clinical syndromes such as the ESS or the low-T3 syndrome. These conditions are characterized by lower circulating T3 levels and minor increases or no changes in the levels of T4 and TSH. ESS is usually associated with high systemic stress resulting from a variety of conditions, including systemic shock, hepatitis, renal disease, and aging (29). ESS-type syndromes are thought to be the result of impaired extrathyroidal peripheral

metabolism, primarily involving the 5′-deiodinases, which convert T4 into metabolically active T3 (20). It is also not clear at present whether ESS-type syndromes represent protective or adaptive physiological mechanisms or are pathological. While stress- or shock-induced animal models for the low-T3 syndrome and ESS have been characterized (5, 20), evidence for genetically determined components associated with ESS is limited (6). Inherited defects in enzymes involved in hormone metabolism (such as the 5′-deiodinases) or T3 and T4 transporter and binding proteins are suggested as possibilities. The discovery of a thyroid hormone phenotype in *frk*/*rak*-deficient animals is unexpected because expression studies and in vitro characterization to date do not support such a function. Although the mechanisms for Frk/rak involvement in thyroid hormone homeostasis or the compensation of the thyroid hormone axis remain unclear, the alteration of thyroid hormone-responsive gene expression suggests a pharmacodynamic effect on the end organs. It is therefore conceivable that subtle genetic defects (such as deficiency of Frk/rak) combined with the appropriate environmental factors could manifest themselves physiologically in ESS-type syndromes.

The results presented here provide the first report on the role of Frk/rak family kinases in development and organ function in vivo. The minimal effect of *frk*/*rak* disruption on epithelial tissues indicates that Frk/rak does not have an essential function in epithelial cell homeostasis, specifically in negative growth regulation and differentiation, as suggested by in vitro experimentation. However, our results do suggest that compensatory events such as the up-regulation of c-*src* may mitigate the effects of Frk/rak loss. The discovery of changes in the thyroid hormone profile of *frk*/*rak*-null mice with symptoms resembling ESS, while surprising, has opened a novel avenue for the investigation of its function. Finally, the generation of mouse models bearing combinations of mutations in other SFKs (*src*, *fyn*, and *yes*) and Frk family kinases (*sik*) coupled with the use of comparative gene expression profiling will help elucidate the physiological functions of Frk/rak family kinases.

ACKNOWLEDGMENTS

We thank Michael Welsh for generously providing the murine Frk/rak antibodies. We thank Anastasia Sowers for technical assistance in the intestinal radiation injury studies. We also thank Anne Latour for generation of targeted ES clones. We are also extremely grateful to Beverly H. Koller for extensive discussion and critical reading of the manuscript.

REFERENCES

1. **Abram, C. L., and S. A. Courtneidge.** 2000. Src family tyrosine kinases and growth factor signaling. Exp. Cell Res. **254:**1–13.
2. **Anneren, C., Reedquist, K. A., J. L. Bos, and M. Welsh.** 2000. GTK, a Src-related tyrosine kinase, induces nerve growth factor independent neurite outgrowth in PC12 cells through activation of the Rap1 pathway. J. Biol. Chem. **275:**29153–29161.
3. **Anneren, C., and M. Welsh.** 2000. Role of the Bsk/Iyk non-receptor tyrosine kinase for the control of growth and hormone production in RINm5F cells. Growth Factors **17:**233–247.
4. **Biedermann, K. A., J. Sun, A. J. Giaccia, L. M. Tosto, and J. M. Brown.** 1991. *scid* mutation in mice confers hypersensitivity to ionizing radiation and a deficiency in DNA double-strand break repair. Proc. Natl. Acad. Sci. USA **88:**1394–1397.
5. **Boelen, A., M. C. Platvoet-ter Schiphorst, O. Bakker, and W. M. Wiersinga.** 1995. The role of cytokines in the lipopolysaccharide-induced sick euthyroid syndrome in mice. J. Endocrinol. **146:**475–483.
6. **Boelen, A., M. A. Maas, C. W. Lowik, M. C. Platvoet, and W. M. Wiersinga.** 1996. Induced illness in interleukin-6 (IL-6) knock-out mice: a causal role of IL-6 in the development of the low 3,5,3′-triiodthyronine syndrome. Endocrinology **137:**5250–5254.
7. **Bosch, T. C. G., T. F. Unger, D. A. Fisher, and R. E. Steele.** 1989. Structure and expression of *STK*, a src-related gene in the simple metazoan *Hydra attenuata*. Mol. Cell. Biol. **9:**4141–4151.
8. **Brown, M. T., and J. A. Cooper.** 1996. Regulation, substrates and functions of src. Biochim. Biophys. Acta **1287:**121–149.
9. **Cance, W. G., R. J. Craven, M. Bergman, L. Xu, K. Alitalo, and E. T. Liu.** 1994. Rak, a novel nuclear tyrosine kinase expressed in epithelial cells. Cell Growth Differ. **5:**1347–1355.
10. **Craven, R. J., W. G. Cance, and E. T. Liu.** 1995. The nuclear tyrosine kinase Rak associates with the retinoblastoma protein pRb. Cancer Res. **55:**3969–3972.
11. **Craven, R. J.** 1996. The biological role of the Rak nuclear tyrosine kinase. Ph.D. thesis. University of North Carolina—Chapel Hill, Chapel Hill.
12. **Grant, S. G., T. J. O'Dell, K. A. Karl, P. L. Stein, P. Soriano, and E. R. Kandel.** 1992. Impaired long-term potentiation, spatial learning, and hippocampal development in *fyn* mutant mice. Science **258:**1903–1910.
13. **Harvat, B. L., A. Wang, P. Seth, and A. M. Jetten.** 1998. Up-regulation of p27Kip1, p21WAF1/Cip1 and p16Ink4a is associated with, but not sufficient for, induction of squamous differentiation. J. Cell Sci. **111:**1185–1196.
14. **Hayat, M. A.** 1970. Principles and techniques of electron microscopy: biological applications, vol. 1. Van Nostrand Reinhold Co., New York, N.Y.
15. **Hendry, J. H., C. S. Potten, and N. P. Roberts.** 1983. The gastrointestinal syndrome and mucosal clogenic cells: relationships between target cell sensitivities, LD50 and cell survival, and their modification by antibiotics. Radiat. Res. **96:**100–112.
16. **Iruvanthi, S., and M. I. Avigan.** 1996. The apical membranes of maturing gut columnar epithelial cells contain enzymatically active form of a newly identified Fyn-related tyrosine kinase. Oncogene **13:**547–559.
17. **Iruvanthi, S., R. Shen, I. H. McKillop, J. H. Lee, J. Resau, and M. I. Avigan.** 1999. A src-related kinase in the brush border membranes of gastrointestinal cells is regulated by c-met. Exp. Cell Res. **250:**86–98.
18. **Iwasa, Y., N. Yokomori, M. Inoue, and T. Onaya.** 1990. Transcriptional regulation of ferritin heavy chain messenger RNA expression by thyroid hormone. Biochem. Biophys. Res. Commun. **167:**1279–1285.
19. **Kaplan, J. M., H. E. Varmus, and J. M. Bishop.** 1990. The src probe contains multiple domains for specific attachment to membranes. Mol. Cell. Biol. **10:**1000–1009.
20. **Kelly, G. S.** 2000. Peripheral metabolism of thyroid hormones: a review. Altern. Med. Rev. **5:**306–333.
21. **Komarova, I., and I. A. Vorob'ev.** 1993. Ultrastructural changes in the cell center during enterocyte differentiation in the mouse. Tsitologiya **35:**36–43.
22. **Komarova, I., and I. A. Vorob'ev.** 1995. The centrosome structure in enterocytes in the histogenesis of the mouse intestine. Ontogenez **26:**390–399.
23. **Lastowska, M. A., D. M. Lillington, A. N. Shelling, I. Cooke, B. Gibbons, B. D. Young, and T. S. Ganesan.** 1994. Fluorescence in situ hybridization analysis using cosmid probes to define chromosome 6q abnormalities in ovarian carcinoma cell lines. Cancer Genet. Cytogenet. **77:**99–105.
24. **Lee, J., Z. Wang, S-M. Luoh, W. I. Wood, and D. T. Scadden.** 1994. Cloning of FRK/RAK, a novel human intracellular SRC-like tyrosine kinase-encoding gene. Gene **138:**247–251.
25. **Levinson, A. D., H. Oppermann, L. Levintow, H. E. Varmus, and J. M. Bishop.** 1978. Evidence that the transforming gene of avian sarcoma virus encodes a protein kinase associated with a phosphoprotein. Cell **15:**561–572.
26. **Llor, X., M. S. Serfas, W. Bie, V. Vasioukhin, M. Polonskaia, J. Derry, C. M. Abbott, and A. L. Tyner.** 1999. BRK/Sik expression in the gastrointestinal tract and in colon tumors. Clin. Cancer Res. **5:**1767–1777.
27. **Lowell, C. A., M. Niwa, P. Soriano, and H. E. Varmus.** 1996. Deficiency of the Hck and Src tyrosine kinases results in extreme levels of extramedullary hematopoiesis. Blood **87:**1780–1792.
28. **Lowell, C. A., and P. Soriano.** 1996. Knockouts of Src-family kinases: stiff bones, wimpy T cells, and bad memories. Genes Dev. **10:**1845–1857.
28a. **Mason, K. A., H. R. Withers, W. H. McBride, C. A. Davis, and J. B. Smathers.** 1989. Comparison of the gastrointestinal syndrome after total-body or total-abdominal irradiation. Radiat. Res. **117:**480–488.
29. **McIver, B., and C. A. Gorman.** 1997. Euthyroid sick syndrome: an overview. Thyroid **7:**125–132.
30. **Miller, L. D., K. S. Park, Q. M. Guo, N. W. Alkharouf, R. L. Malek, N. H. Lee, E. T. Liu, and S. Y. Cheng.** 2001. Silencing of Wnt signaling and activation of multiple metabolic pathways in response to thyroid hormone-stimulated cell proliferation. Mol. Cell. Biol. **21:**6626–6639.
31. **Miller, S. A., D. D. Dykes, and H. F. Poelesky.** 1988. A simple salting out procedure for extracting DNA from human nucleated cells. Nucleic Acids Res. **16:**12–15.
32. **Mitchell, P. J., K. T. Barker, J. E. Martindale, T. Kamalati, P. N. Lowe, M. J. Page, B. A. Gusterson, and M. R. Crompton.** 1994. Cloning and characterization of cDNA encoding a novel non-receptor tyrosine kinase, brk, expressed in human breast tumors. Oncogene **9:**2383–2390.
33. **Mitchell, P. J., K. T. Barker, J. Shipley, and M. R. Crompton.** 1997. Characterization and chromosome mapping of the human non-receptor tyrosine kinase gene, brk. Oncogene **15:**1497–1502.
34. **Mohn, A., and B. H. Koller.** 1995. Genetic manipulation of embryonic stem

cells, p. 143–184. *In* D. M. Glover and B. D. Hanes, DNA cloning, 4th ed. Oxford University Press, New York, N.Y.

35. **Negrini, M., S. Sabbioni, L. Possati, S. Rattan, A. Corallini, G. Barbanti-Brodano, and C. M. Croce.** 1994. Suppresion of tumorigenicity of breast cancer cells by microcell-mediated chromosome transfer: studies on chromosome 6 and 11. Cancer Res. **54:**1331–1336.
36. **Nussenzweig, A., K. Sokol, P. Burgman, L. Li, and G. C. Li.** 1997. Hypersensitivity of Ku80-deficient cell lines and mice to DNA damage. The effects of ionizing radiation on growth, survival, and development. Proc. Natl. Acad. Sci. USA **94:**13588–13593.
37. **Oberg-Welsh, C., and M. Welsh.** 1995. Cloning of BSK, a murine FRK/RAK homologue with a specific pattern on tissue distribution. Gene **152:**239–242.
38. **Oberg-Welsh, C., C. Anneren, and M. Welsh.** 1998. Mutation of C-terminal tyrosine Y497/Y504 of the Src-family member Bsk/Iyk decreases NIH3T3 cell proliferation. Growth Factors **16:**111–124.
39. **Ottilie, S., F. Raulf, A. Barnekow, G. Hannig, and M. Schartl.** 1992. Multiple src-related kinase genes, srk1–4, in the fresh water sponge Spongilla lacustris. Oncogene **7:**1625–1630.
40. **Ouafik, L., V. May, D. W. Saffen, and B. A. Eipper.** 1990. Thyroid hormone regulation of peptidylglycine alpha-amidating monooxygenase expression in anterior pituitary gland. Mol. Endocrinol. **4:**1497–1505.
41. **Phillips, J., and J. H. Eberwine.** 1996. Antisense RNA amplification: a linear amplification method for analyzing the mRNA population from single living cells. Methods **10:**283–288.
42. **Robinson, D. R., Y.-M. Wu, and S.-F. Lin.** 2000. The protein tyrosine kinase family of the human genome. Oncogene **19:**5548–5557.
43. **Sheng, Z. M., A. Marchetti, F. Buttitta, M. H. Champerne, D. Campani, M. Bistocchi, R. Lidreau, and R. Callahan.** 1996. Multiple regions of chromosome 6q affected by loss of heterozygosity in primary human breast carcinomas. Br. J. Cancer **73:**144–147.
44. **Soriano, P., C. Montgomery, R. Geske, and A. Bradley.** 1991. Targeted disruption of the c-src proto-oncogene leads to osteopetrosis in mice. Cell **64:**693–702.
45. **Stehelin, D., H. Varmus, J. Bishop, and P. Vogt.** 1976. DNA related to transforming gene(s) of avian sarcoma viruses is present in normal avian DNA. Nature **260:**170–173.
46. **Stein, P. L., H. Vogel, and P. Soriano.** 1994. Combined deficiencies of Src, Fyn, and Yes tyrosine kinases in mutant mice. Genes Dev. **8:**1999–2007.
47. **Takahashi, F., S. Endo, T. Kojima, and K. Saigo.** 1996. Regulation of cell-cell contacts in developing Drosophila eyes by Dsrc4–1, a new, close relative of vertebrate c-src. Genes Dev. **10:**1645–1656.
48. **Thomas, S. M., P. Soriano, and A. Imamoto.** 1995. Specific and redundant roles of Src and Fyn in organizing the cytoskeleton. Nature **376:**267–271.
49. **Thomas, S. M., and J. S. Brugge.** 1997. Cellular functions regulated by SRC family kinases. Annu. Rev. Cell Dev. Biol. **13:**513–609.
50. **Thuveson, M., D. Albrecht, G. Zurcher, A.-C. Andres, and A. Ziemiecki.** 1995. IYK, a novel intracellular protein tyrosine kinase differentially expresses in the mouse mammary gland and intestine. Biochem. Biophys. Res. Commun. **209:**582–589.
51. **Tian, J. Q., and A. Quaroni.** 1999. Involvement of p21 (WAF1/Cip1) and p27 (Kip1) in intestinal epithelial cell differentiation. Am. J. Physiol. **276:**1245–1258.
52. **Trucco, C., V. Rolli, F. J. Oliver, E. Flatter, M. Masson, F. Dantzer, C. Niedergang, B. Dutrillaux, et al.** 1999. A dual approach in the study of poly (ADP-ribose) polymerase: in vitro random mutagenesis and generation of deficient mice. Mol. Cell. Biochem. **193:**53–60.
53. **Vasioukhin, V., M. S. Serfas, E. Y. Siyanova, M. Polonskaja, V. J. Costigan, B. Liu, A. Thomason, and L. A. Tyner.** 1995. A novel intracellular epithelial cell tyrosine kinase is expressed in the skin and gastrointestinal tract. Oncogene **10:**349–357.
54. **Vasioukhin, V., and L. A. Tyner.** 1997. A role of the epithelial cell specific tyrosine kinase Sik during keratinocyte differentiation. Proc. Natl. Acad. Sci. USA **94:**14477–14482.